

Identification of Sea Surface Temperature Anomaly during Earthquake in Southern Java Island using Google Earth Engine Datasets

Alfi Nur Rusydi^{1*}, Ferryati Masitoh², Tasya Salsabila Adzkiya¹

¹Faculty of Fisheries and Marine Science, Universitas Brawijaya, Malang, Indonesia

²Department of Geography, Faculty of Social Science, Universitas Negeri Malang, Malang, Indonesia

Received : 2021-08-05

Revised : 2021-10-17

Accepted: 2023-02-16

Key words: earthquake;
Google Earth Engine; SST;
sea surface; temperature

Correspondent email:
alfi.nurrusydi@ub.ac.id

Abstract The certainty of Sea Surface Temperature (SST) anomaly during earthquakes in Java Island was still not clear identified. This research tried to identify any possibilities of SST anomaly during earthquake in Southern Java Island. It used Google Earth Engine datasets including daily NOAA Climate Data Record (CDR) - Woods Hole Oceanographic Institution (WHOI): Sea Surface Temperature Version 2 which has resolution of 0.25 arc degrees for 20 years and processed them to depict SST trends in pre-earthquake and post-earthquake situation. The statistic test of t-Test Paired Two Sample was also applied to certain the significant difference of SST in both situations. SST fluctuation during the earthquake was still inconsistent and unclear to consider as an anomaly. There were other complicated factors excluding earthquake to influence SST fluctuation. The earthquake did not trigger directly to fluctuate SST, even not to make it being an anomaly.

©2023 by the authors. Licensee Indonesian Journal of Geography, Indonesia.

This article is an open access article distributed under the terms and conditions of the Creative Commons Attribution (CC BY NC) license <https://creativecommons.org/licenses/by-nc/4.0/>.

1. Introduction

Java Island is the most experienced island by tectonic earthquake (Marfai et al., 2008) and is the most people population density island in Indonesia (Pasari et al., 2021). Mostly epicenters position of Java Island's earthquake are in southern sea of the island (Harig et al., 2020) belonging to subduction lane of Australia and Eurasia plates. There are 2470 earthquakes M=3-7 occurrences centered in southern sea of Java along the period of 2000-2021 (USGS-NEIC, 2020).

Sea Surface Temperature (SST) fluctuation and anomaly probably occurred during the earthquake (Ma et al., 2008; Tüfekçi & Akman, 2005). Pre-earthquake might also trigger LST anomalies based on remote sensing data but LST could not be earthquake precursors without a global scale monitoring system for statistical detection of robust anomalous geophysical signals (Bhardwaj et al., 2017) Temperature anomaly was able to be identified using remote sensing technology (Tamiminia et al., 2020). NOAA satellite was often used for SST anomaly identification (Hosoda, 2010). It has wide scanning scope which 1 pixel of the image represents 1,1 Km² area and the global Root Mean Square (RMS) error of the SST data ranged from 0,6-0,7°K (Guan & Kawamura, 2004). NOAA satellite imagery becomes the appropriate main data for SST identification around southern of Java Island which has 128.297 km² area. This research used Google Earth Engine for NOAA satellite imagery datasets processing. In detail, it used NOAA Climate Data Record (CDR) of Sea Surface Temperature - WHOI since it provides a high-quality Climate Data Record (CDR) of sea surface temperature over ice-free oceans. The SST data were identified by combination

of diurnal variability model and AVHRR observations of sea surface temperature. It contains a 3-hourly data from January 1988 to present. By spatial resolution of 27830 meters, it can also present the whole scope of research area in Southern Java Island (Clayson et al., 2016). Google Earth Engine is the cloud computing platform developed by Google, Inc which was optimally utilized to support earth analysis (Tamiminia et al., 2020). Limitation of a platform in downloading, storing and big data processing could be handled by GEE (Shetty et al., 2021). GEE consisted of two main components working together which are Google Earth Engine Explorer (EE) (for data presentation) and Google Earth Engine Playground (EEP). Google EEP is an Application Programming Interfaces (API) JavaScript used for uploading, big data analyzing of satellite imagery, and complex geostatistical and geospatial processing (Shetty et al., 2021).

Temperature anomaly has various definition among researchers (Efimov & Barabanov, 2017; Kiselev, 2016; Shi et al., 2016). It refers to unique temperature condition which appear at hours before earthquake and after earthquake (Akhoondzadeh, 2013). SST anomaly triggered by earthquake in southern Java Island did not be identified yet. This research tries to identify SST anomaly at before and during earthquake in southern Java Island in 20 years starting from 2000-2021. Earth surface temperature changes at a few moments before earthquake had been reported (Cicerone et al., 2009). Temperature anomaly and earthquake relationship did not defined yet clearly (Pavlidou et al., 2019).

SST and earthquake relationship was not be able to well defined yet since there was not consistently SST fluctuation pattern triggered by earthquake. There was few different

between SST before and SST during the earthquake. Temperature anomaly was well identified before and after the earthquake in Saravan, Iran by using MODIS-Aqua satellite imagery (Khalili *et al.*, 2020). The research compared the surface temperature before and after earthquake and explained the increased temperature on 3-7 days after earthquake (Khalili *et al.*, 2020). That increasing was only triggered by the earthquake, not by seasonal weather pattern (Khalili *et al.*, 2020).

2. Methods

Data

The previous research related to temperature anomaly and earthquake activity in Middle Asia used 7 years data series (Tronin, 2000). Even, another research used 30 years data series (1979-2008) in China (Xiong & Shen, 2017). The earthquake data used in this research is 20 years data series of USGS starting from 2000-2021. The data contains epicenter location (longitude and latitude), magnitude, and depth. It was sorted by earthquake occurrence with $M = \pm 6$ only. Temperature anomaly triggered by earthquake will be more sensitive to be occurred if the $M = > 4,7$ and earthquake propagation radius is up to 500 Km (Tronin, 2000). SST was generated by

dataset of NOAA Climate Data Record (CDR) - Woods Hole Oceanographic Institution (WHOI): Sea Surface Temperature Version 2 which has resolution of 0.25 arc degrees. SST was generated by modeling the diurnal variability and warming correction in combination with AVHRR observations of sea surface temperature (Clayson *et al.*, 2016).

Data Processing

Epicenters was plotted on the base map using Quantum GIS software based on their longitude and latitude to show spatial distribution of those epicenters. An Area of Interest (AOI) was created to border the study area following epicenters distribution scope (see Figure 1). Not all SST data were presence inside AOI. NOAA satellite provided raw SST data of the area only located more than 80 or 90 km from coastline. Epicenters $M = \pm 6$ located less than 80 or 90 km from coastline had not raw SST data. There are 7 epicenters $M = \pm 6$ inside SST area. They were excluded to be involved in the analysis. This research used daily SST along one month including at before, during, and after earthquake occurred. All research data were analyzed on those 7 epicenters. Earthquake occurrences detail was shown in Table 1.

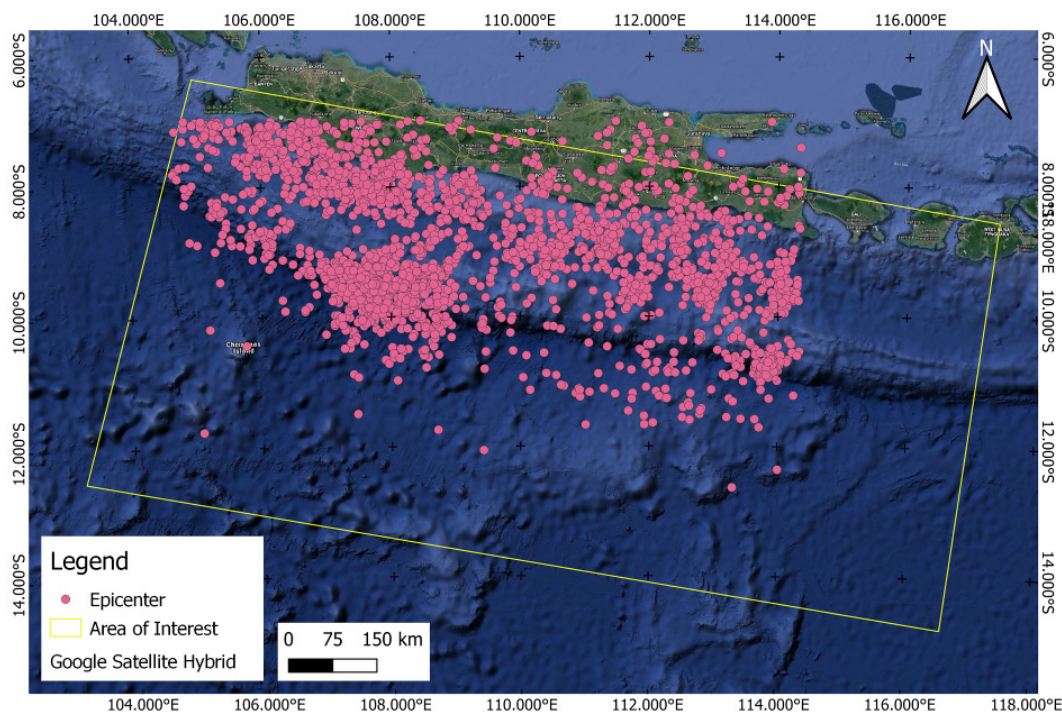


Figure 1. AOI of Southern Java Island Earthquakes in Period 2000-2021

Table 1. Epicenters with $M = \pm 6$ in Period of 2000-2021 Inside AOI

Point	Date	Longitude	Latitude	Magnitude	Depth
1	17 July 2006	107,76	-9,087	6	10
2	17 July 2006	107,419	-9,284	7,7	20
3	17 July 2006	108,319	-9,42	6,1	21
4	21 September 2006	110,365	-9,05	6	25
5	7 September 2009	110,628	-10,198	6,2	23
6	3 April 2011	107,693	-9,848	6,7	14
7	3 September 2012	113,931	-10,708	6,1	14

Source : United State Geological Survey (USGS)

SST was generated using algorithms and codes applied to Google Earth Engine datasets (https://code.earthengine.google.com/?accept_repo=users/alfinurrusydi/sst). *var_dataset* is a code for importing 'NOAA/CDR/SST_WHOI/V2' available in GEE dataset catalog. The data filtering was then implemented based on time period using *ee.Filter.Date* command. It was adjusted to the time before and after earthquake occurrence. Dataset of 'NOAA/CDR/SST_WHOI/V2' has only 1 band which is *sea_surface_temperature* (unit in Celsius degree) (Clayson et al., 2016). Each Digital Number value of it represents as Optimum Interpolation Sea Surface Temperature (OISST) with minimum value of -1,79 °C and maximum value of 35 °C.

Map.setCenter(112.47, -8.46, 2) is a command to center the coordinate point of research area (Area of Interest/AOI). Command of *dataset2.filterBounds(table)* was used to border the AOI polygon as research area. *Table* in that command showed the polygon geometry data in GEE. SST trend in 1 month required long data series and in GEE, then *ee.Filter.date* command was implemented by inputting both start and end date. For representing SST trends into the graphic, it can be showed in GEE console through *ui.Chart.image.series* command. The algorithms and codes used are presented as Figure 2:

Mean daily SST along one month of earthquake were presented in bar graph to identify SST anomaly around epicenter (the earthquake data can be downloaded from URL link as follow: <https://search.earthdata.nasa.gov/>) inside certain radius. That certain radius distance was in kilometers and was used as boundary for picking SST data samples. We use this radius to pick samples of SST values. Another previous research assumed that temperature fluctuation occurred locally and be isolated (Pavlidou et al., 2016). Temperature anomaly appeared at 6-24 days before earthquake and it was

still going on for one week after earthquake (Tronin, 2000). Anomaly temperature occurred at one or two months before earthquake and it would be more distinct in near to epicenter (Xiong & Shen, 2017). Mostly temperature anomalies were detected in near area to epicenter (Pavlidou et al., 2019). Spatial distribution of SST was identified visually on SST maps. For statistical test, ten SST data samples for each epicenter were taken randomly inside that certain radius. Statistical testing using t-test was applied to certain the significantly difference of SST on one day before and during the earthquake.

3. Result and Discussion

SST anomaly triggered by earthquake was identified through significant SST difference. This research identified SST fluctuation and excluded sea subsurface temperature influence. Data processing of NOAA satellite imagery showed that SST area did not coincide with all AOI borders. There are 7 epicenters $M=\pm 6$ inside that area (see Figure 2). They are 4 epicenters of 2006 distributed separately in southern West Java and East Java; 1 epicenter of 2009 in southern East Java; 1 epicenter of 2011 in southern West Java; and 1 epicenter of 2012 in southern East Java.

SST distribution around epicenters was spatially different which the higher SST, the redder area is shown (see Figure 3). There is visually different between SST before and during the earthquake. Mean SST fluctuation along one month of earthquake indicated inconsistent SST pattern (see Figure 4). Mean SST fluctuations for earthquakes $M=\pm 6$ of 17 July 2006, 7 September 2009, 3 April 2011 and 3 September 2012 tended to decrease and they returned to increase on one day after earthquake occurrences, respectively. Different SST fluctuations are shown by earthquakes of 21 September 2006 which SST continued to increase on few days before and after earthquake.

SST Source Code	One Month SST Trend Source Code
<pre>var dataset = ee.ImageCollection('NOAA/CDR/SST_WHOI/V2') .filter(ee.Filter.date('2006-07-17')); var seaSurfaceTemperature = dataset.select('sea_surface_temperature'); var visParams = { min: 0.0, max: 30.0, palette: ['040274', '040281', '0502a3', '0502b8', '0502ce', '0502e6', '0602ff', '235cb1', '307ef3', '269db1', '30c8e2', '32d3ef', '3be285', '3ff38f', '86e26f', '3ae237', 'b5e22e', 'd6e21f', 'fff705', 'ffd611', 'ffb613', 'ff8b13', 'ff6e08', 'ff500d', 'ff0000', 'de0101', 'c21301', 'a71001', '911003'], }; Map.setCenter(112.47, -8.46, 2); Map.addLayer(seaSurfaceTemperature, visParams, 'Sea Surface Temperature');</pre>	<pre>var dataset2 = ee.ImageCollection('NOAA/CDR/SST_WHOI/V2'); var temps2 = dataset2.filterBounds(table) .filter(ee.Filter.date('2006-07-01', '2006-07-31')); var seaSurfaceTemperature02 = dataset2.select('sst'); var tempTimeSeries2 = ui.Chart.image.series({ imageCollection: temps2, region: table, reducer: ee.Reducer.mean(), scale: 10000, xProperty: 'system:time_start' }); tempTimeSeries2.setChartType('ScatterChart'); tempTimeSeries2.setOptions({ title: 'SST July 2006', vAxis: {title: 'Temperature'}, hAxis: {title: 'Date'}, lineWidth: 1, pointSize: 4, }); print(tempTimeSeries2);</pre>

Figure 2. Example of SST Source Code

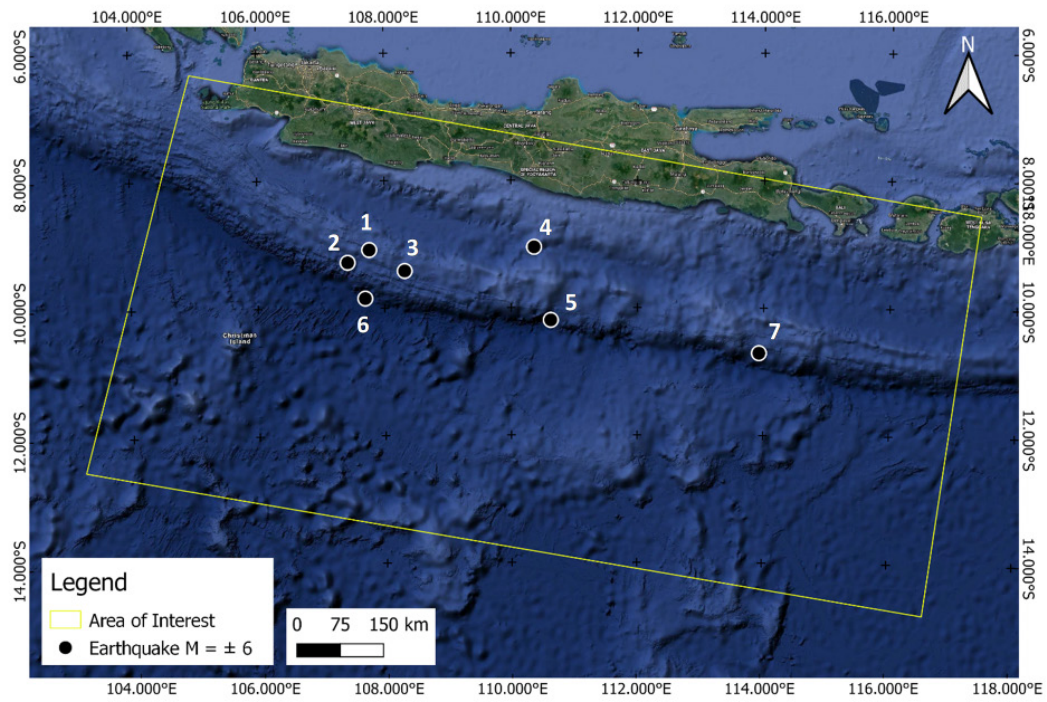
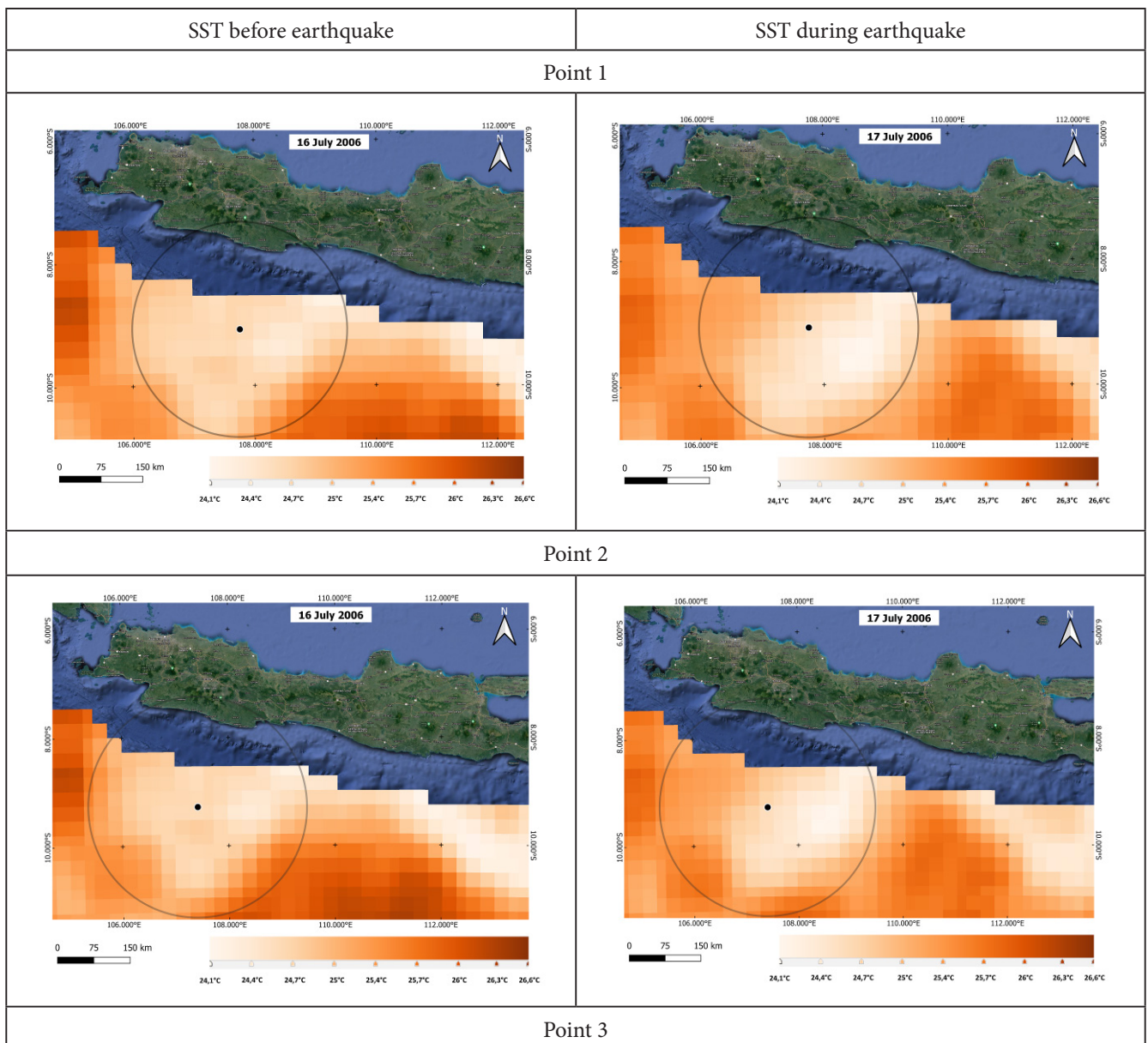
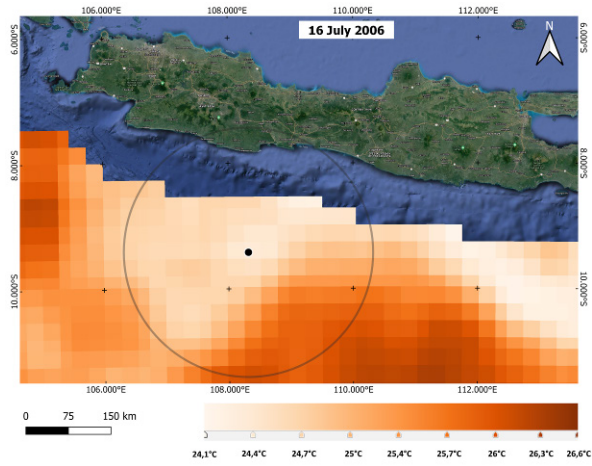


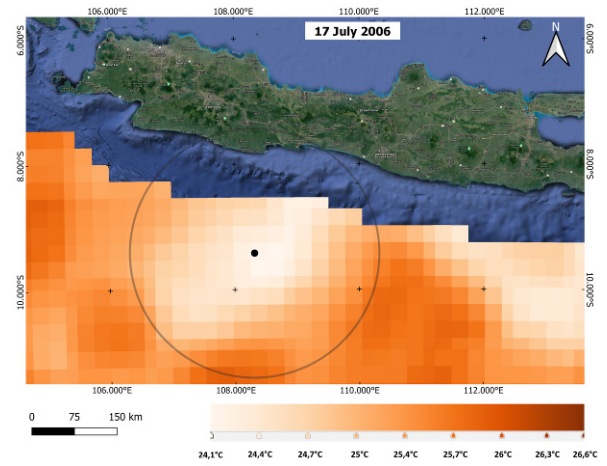
Figure 2. AOI of Southern Java Island Earthquakes $M=\pm 6$ in Period 2000-2021



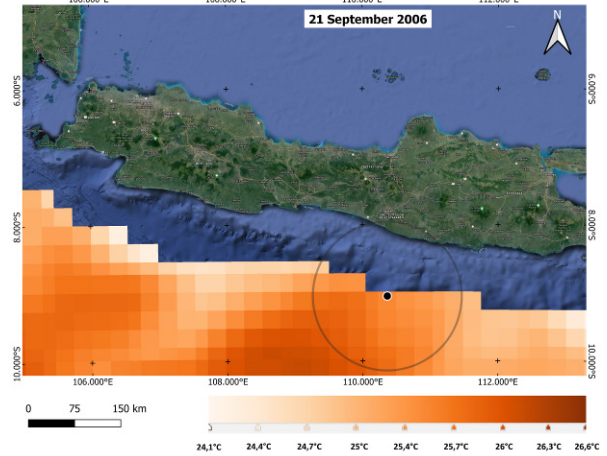
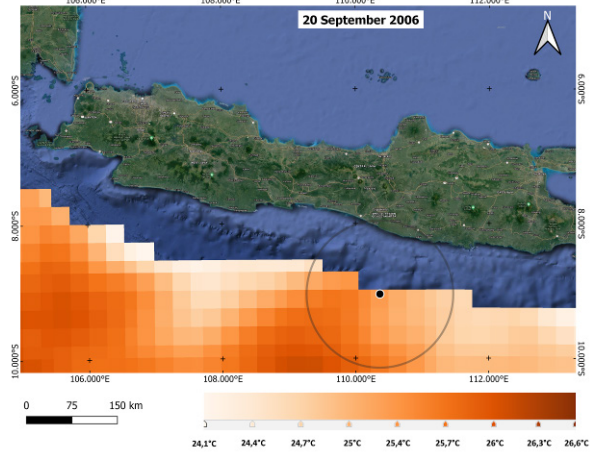
SST before earthquake



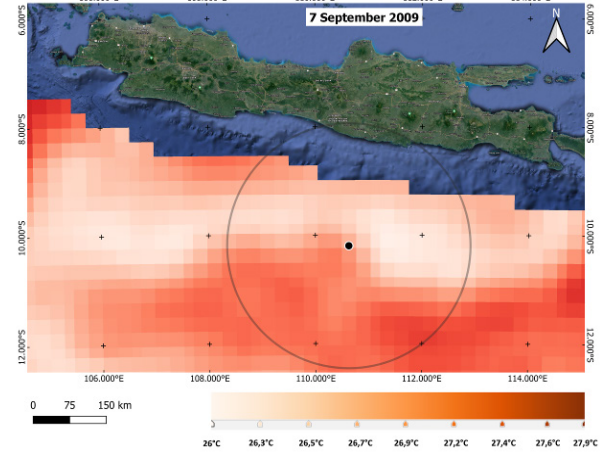
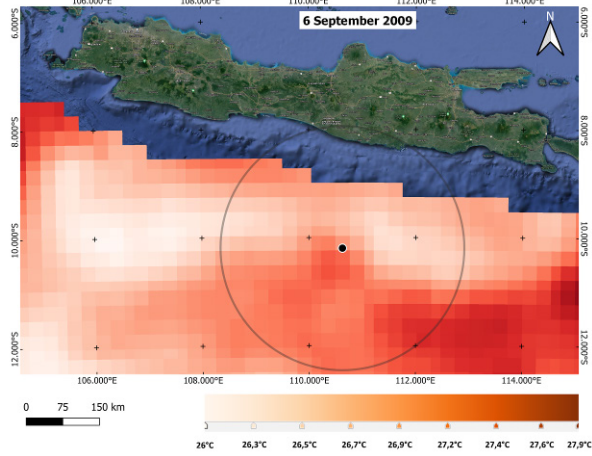
SST during earthquake



Point 4



Point 5



Point 6

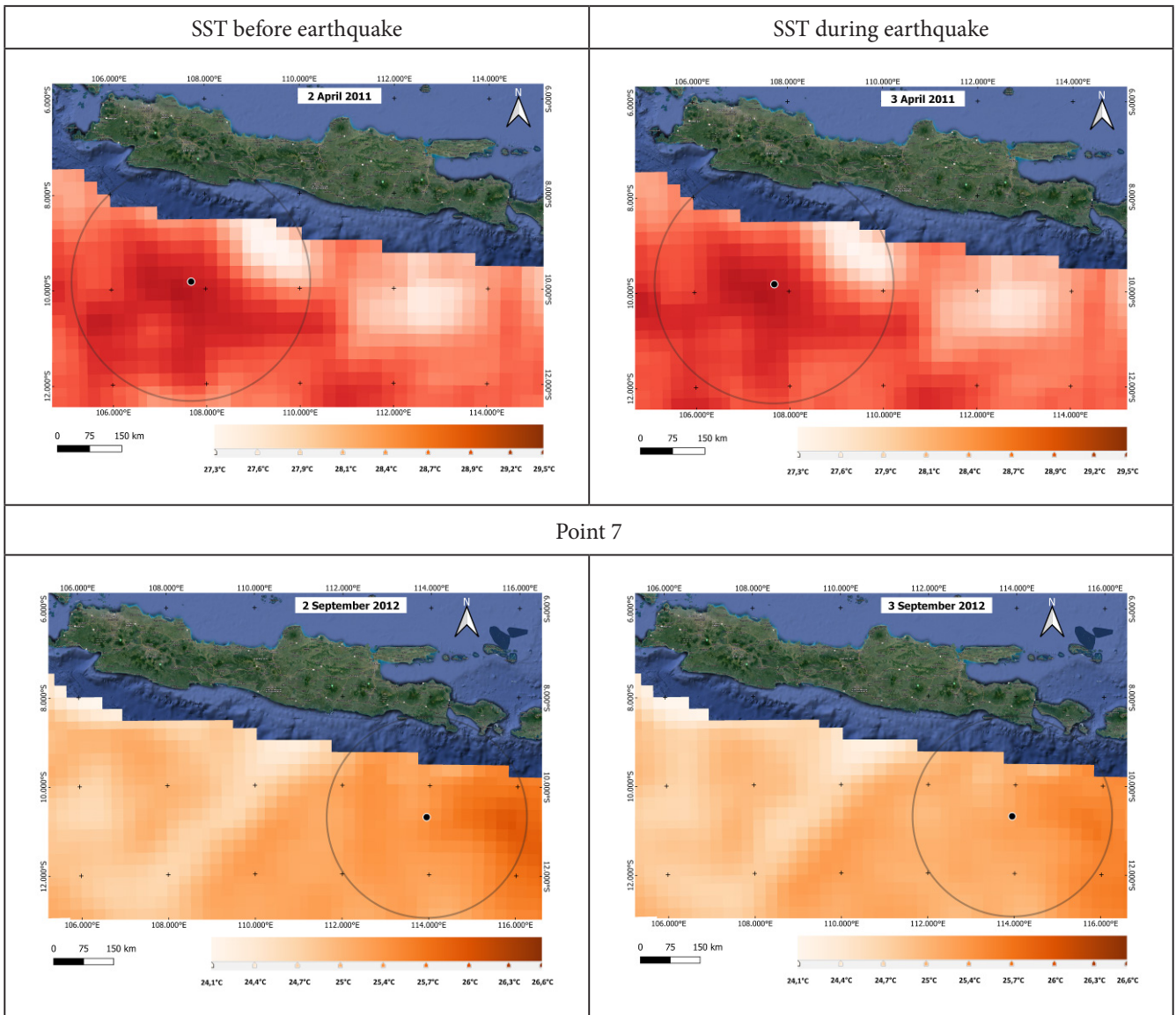
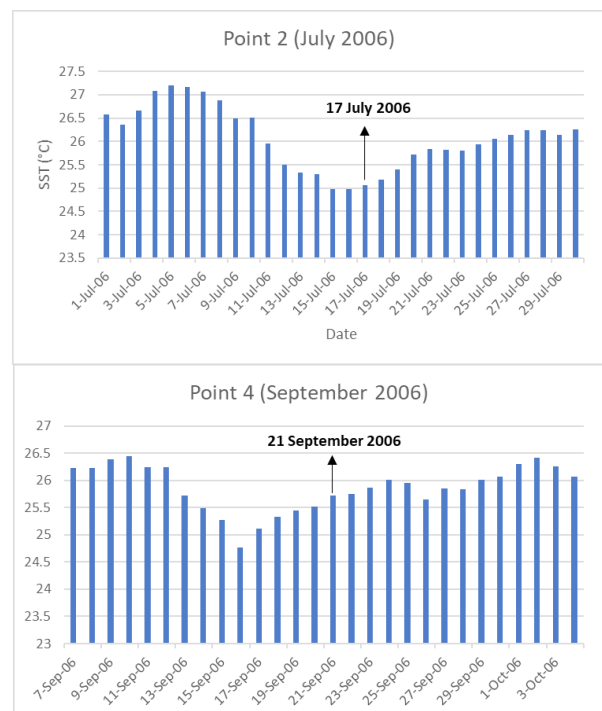
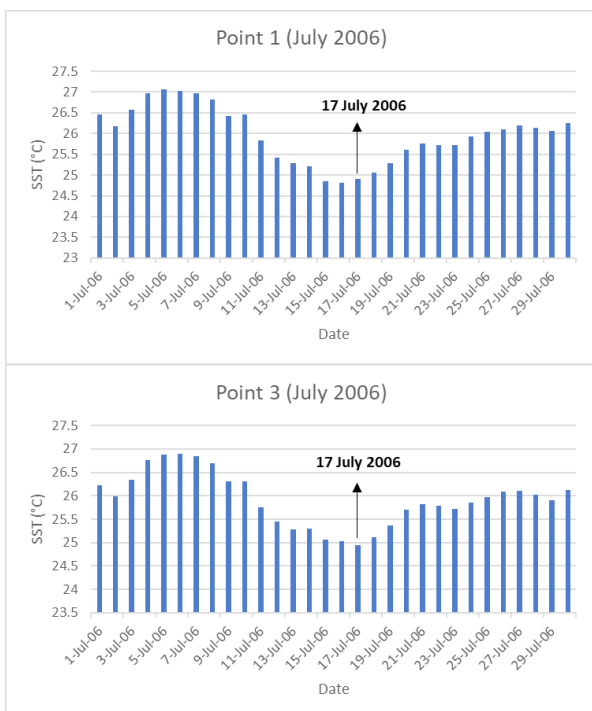


Figure 3. SST of Southern Java Island Before and During Earthquakes $M=±6$



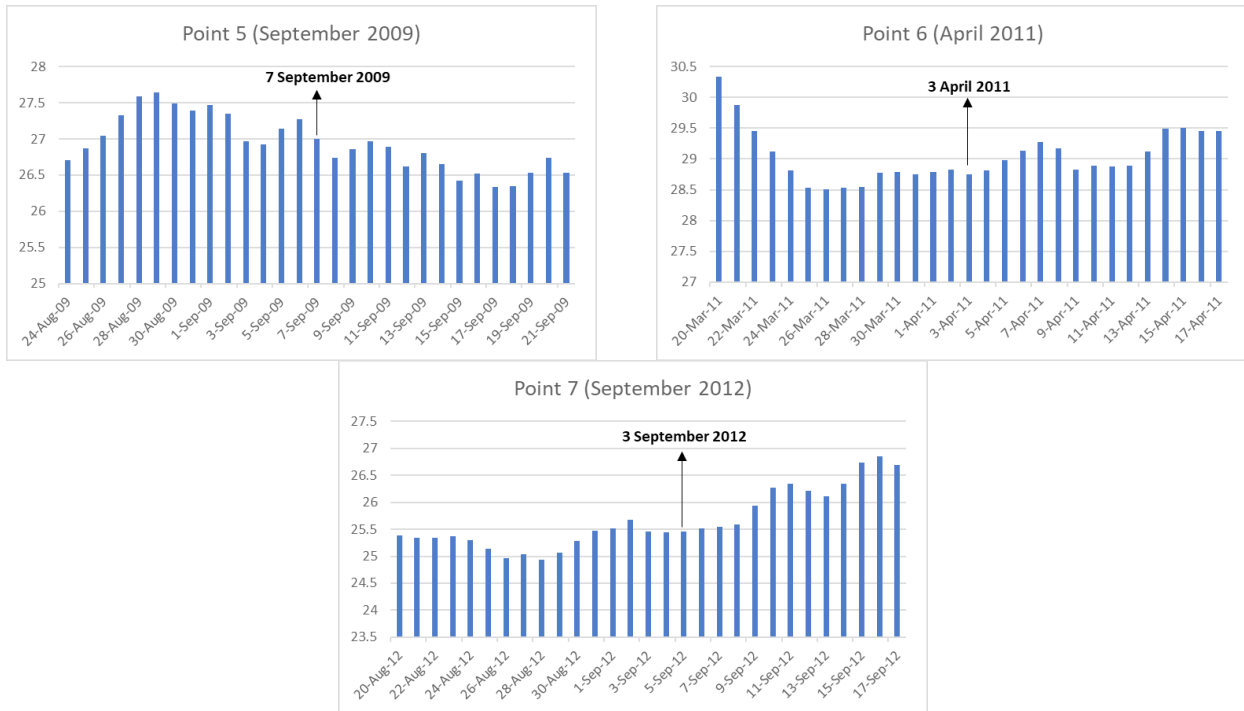


Figure 4. One Month Mean SST Fluctuation of Earthquake $M=\pm 6$ Inside AOI

The inconsistent pattern of SST fluctuation (see Figure 4) could be influenced by related factors. The decreasing SST trend could be caused by vertical mixed sea water column (Subrahmanyam, 2015). Earthquake vibration including foreshock, mainshock and aftershock triggered surface water to move down into subsurface water column, while subsurface water was forced to move up onto surface (Kopnichev & Sokolova, 2018; Zhigalin et al., 2014). Warm surface water heated by sun radiation moved down and it changed subsurface water temperature (Rogachev et al., 2000). Cold subsurface water moved up and it decreased surface water temperature. The increasing SST trend during earthquake was the effect of greenhouse gases release since of induction pressure before the earthquake (Choudhury et al., 2006). Greenhouse gases consisting of CH_4 and CO_2 increased by tens of thousands times around epicenter area (Qiang et al., 1999). The increasing SST trend around epicenter was also as the consequence of not released mechanical energy accumulation stored in earth crust during the earthquake (Freund, 2003). Then, the energy had changed into other energy forms, such as electrical energy and thermal energy (Freund, 2003). Air ionization as radon radiation effect from active fault and fracture could contribute in changing both air and earth surface temperature (Pulinets et al., 2006).

Statistical test considering spatial and temporal parameters was involved into evaluating research findings related to thermal anomaly and earthquake occurrence (Pavlidou et al., 2019). This research used statistic test to certain that SST acquired at both two conditions; before and during earthquake were significantly different. The previous research proved that there was less precise and unclear correlation between thermal anomaly and earthquake (Eneva, 2008) since temperature anomaly was dominantly influenced by atmosphere condition including cloud cover, the presence of satellite imagery data gaps and mosaicking of orbits of data, not came from the earthquake (Blackett et al., 2011). The previous research explained that in the fact, the temperature anomaly comes from the presence of cloud cover and data gaps observed based on MODIS satellite imagery for full six years (2001-2006) in Gujarat, India which affects warmer areas (Blackett et al., 2011). T-test as parametrical statistic test was chosen since the data was normally distributed and there was no outlier for all data distribution. T-test result shows that T-table was higher than T-value (Table 2). It means that pre-earthquake SST and post-earthquake SST was significantly different (H_0 was rejected), in spite of few SST values difference. The difference was strengthened by SST maps presentation. Temperature of both situations around epicenter was spatially different showed by different color gradation symbol.

Table 2. Statistic test of t-Test Paired Two Sample of SST for Means

Result	Before	During
Mean	25.80249106	25.9058263
Variance	1.894444444	1.799583263
Observations	70	70
Pearson Correlation	0.990820312	
df	69	
t Stat	-4.580512465	
P(T<=t) two-tail	0.0000203596308983794	
t Critical two-tail	1.995468931	

Source : secondary data processing

Comparing SST differences by maps, graphic chart, statistic test of both conditions showed that SST anomaly triggered by earthquake $M = \pm 6$ in Java Island did not be well explained since of inconsistent SST fluctuation among them. Unclear SST anomaly was also found by the previous research related to long wave radiation variability of infrared spectrum for earthquake in Andaman Island, Sumatera, Indonesia (Ouzounov et al., 2007). Unclear of SST anomaly was influenced by air ionization near to soil surface and latent heat changes as air temperature and humidity changes impact (Ouzounov et al., 2007). Unclear of SST anomaly could appear since of influence factors such as surface spectral emissivity, atmosphere spectral transmission, surface temperature (spatial and temporal changes), monitoring condition (temporal variation in satellite zenithal angle), and so on (Genzano et al., 2015). Pixel restrictiveness of satellite imagery for study area probably contributed to unclarity temperature anomaly (Akhoondzadeh, 2013). Unclear of temperature anomaly as limitation of NOAA satellite resolution also occurred on earthquake of $M=7,2$ in Baja California (Jie & Guanmeng, 2013).

4. Conclusion

SST anomaly triggered earthquakes in southern Java Island resulted unclear pattern. SST before and after earthquake situation fluctuated in various different patterns. Unclear of SST pattern was more influenced by complicated SST fluctuation factors. SST before and during the earthquake was significant different statistically, but there was not exact reason to explain clearly how SST became fluctuated during earthquakes in Java Island. SST fluctuation during the earthquake in Java Island could not be considered as clear SST anomaly due to complicated other influence factors to the fluctuation outside the earthquake. More total earthquakes and SST data series would be required for delivering different result of the further research. The different kind of satellite imagery may also clarify scientific explanation of unclear SST anomaly during the earthquake in Java Island.

Acknowledgement

This research is funded by Non-tax State Revenue (PNBP) budget of Faculty of Fisheries and Marine Science, University of Brawijaya.

References

- Akhoondzadeh, M. (2013). A comparison of classical and intelligent methods to detect potential thermal anomalies before the 11 August 2012 Varzeghan, Iran, earthquake ($M_w 6.4$). *Natural Hazards and Earth System Science*, 13(4), 1077–1083. <https://doi.org/10.5194/nhess-13-1077-2013>
- Bhardwaj, A., Singh, S., Sam, L., Joshi, P. K., Bhardwaj, A., Martín-Torres, F. J., & Kumar, R. (2017). A review on remotely sensed land surface temperature anomaly as an earthquake precursor. *International Journal of Applied Earth Observation and Geoinformation*, 63, 158–166. <https://doi.org/https://doi.org/10.1016/j.jag.2017.08.002>
- Blackett, M., Wooster, M. J., & Malamud, B. D. (2011). Exploring land surface temperature earthquake precursors: A focus on the Gujarat (India) earthquake of 2001. *Geophysical Research Letters*, 38(15), 1–7. <https://doi.org/10.1029/2011GL048282>
- Choudhury, S., Dasgupta, S., Saraf, A. K., & Panda, S. (2006). Remote sensing observations of pre-earthquake thermal anomalies in Iran. *International Journal of Remote Sensing*, 27(20), 4381–4396. <https://doi.org/10.1080/01431160600851827>
- Cicerone, R. D., Ebel, J. E., & Britton, J. (2009). A systematic compilation of earthquake precursors. *Tectonophysics*, 476(3–4), 371–396. <https://doi.org/10.1016/j.tecto.2009.06.008>
- Clayson, C. A., Brown, J., & NOAA CDR Program. (2016). *NOAA Climate Data Record (CDR) of Sea Surface Temperature - WHOI, Version 2*. NOAA National Climatic Data Center. <https://doi.org/doi:10.7289/V5FB510W>
- Efimov, V. V., & Barabanov, V. S. (2017). Anomalies of the Black Sea surface temperature and modeling of intense cold anomaly formation in September 2014. *Izvestiya, Atmospheric and Oceanic Physics*, 53(3), 343–351. <https://doi.org/10.1134/S0001433817030057>
- Eneva, M. (2008). *Eneva M., D. Adams, N. Wechsler, Y. Ben-Zion, and O. Dor, Thermal Properties of Faults in Southern California from Remote Sensing Data, Final Report to NASA, 2008*.
- Freund, F. T. (2003). Rocks that crackle and sparkle and glow: Strange pre-earthquake phenomena. *Journal of Scientific Exploration*, 17(1), 37–71.
- Genzano, N., Filizzola, C., Paciello, R., Pergola, N., & Tramutoli, V. (2015). Robust Satellite Techniques (RST) for monitoring earthquake prone areas by satellite TIR observations: The case of 1999 Chi-Chi earthquake (Taiwan). *Journal of Asian Earth Sciences*, 114, 289–298. <https://doi.org/10.1016/j.jseaes.2015.02.010>
- Guan, L., & Kawamura, H. (2004). Merging satellite infrared and microwave SSTs: Methodology and evaluation of the new SST. *Journal of Oceanography*, 60(5), 905–912. <https://doi.org/10.1007/s10872-005-5782-5>
- Harig, S., Immerz, A., Weniza, Griffin, J., Weber, B., Babeyko, A., Rakowsky, N., Hartanto, D., Nurokhim, A., Handayani, T., & Weber, R. (2020). The Tsunami Scenario Database of the Indonesia Tsunami Early Warning System (InaTEWS): Evolution of the Coverage and the Involved Modeling Approaches. *Pure and Applied Geophysics*, 177(3), 1379–1401. <https://doi.org/10.1007/s00024-019-02305-1>
- Hosoda, K. (2010). A review of satellite-based microwave observations of sea surface temperatures. *Journal of Oceanography*, 66(4), 439–473. <https://doi.org/10.1007/s10872-010-0039-3>
- Jie, Y., & Guanmeng, G. (2013). Preliminary analysis of thermal anomalies before the 2010 Baja California M7.2 earthquake. *Atmosfera*, 26(4), 473–477. [https://doi.org/10.1016/S0187-6236\(13\)71089-0](https://doi.org/10.1016/S0187-6236(13)71089-0)
- Khalili, M., Abdollahi Eskandar, S. S., & Alavi Panah, S. K. (2020). Thermal anomalies detection before Saravan earthquake (April 16th, 2013, $M_w = 7.8$) using time series method, satellite, and meteorological data. *Journal of Earth System Science*, 129(1). <https://doi.org/10.1007/s12040-019-1286-3>
- Kiselev, B. V. (2016). Studying randomness and determinism in surface temperature anomaly indices using the recurrence plot method. *Izvestiya, Atmospheric and Oceanic Physics*, 52(1), 33–36. <https://doi.org/10.1134/S0001433816010059>
- Kopnichev, Y. F., & Sokolova, I. N. (2018). Characteristics of Seismicity in the Areas of Large Water Reservoirs and Waterfalls: The Role of Effects from Additional Load and Permanent Vibration. *Seismic Instruments*, 54(2), 230–238. <https://doi.org/10.3103/S0747923918020081>
- Ma, W., Ma, W., Zhao, H., & Li, H. (2008). Temperature changing process of the Hokkaido (Japan) earthquake on 25 September 2003. *Natural Hazards and Earth System Science*, 8(5), 985–989. <https://doi.org/10.5194/nhess-8-985-2008>
- Marfai, M. A., King, L., Singh, L. P., Mardiatno, D., Sartohadi, J., Hadmoko, D. S., & Dewi, A. (2008). Natural hazards in Central Java Province, Indonesia: An overview. *Environmental Geology*, 56(2), 335–351. <https://doi.org/10.1007/s00254-007-1169-9>
- Ouzounov, D., Liu, D., Chunli, K., Cervone, G., Kafatos, M., & Taylor, P. (2007). Outgoing long wave radiation variability from IR satellite data prior to major earthquakes. *Tectonophysics*,

- 431(1), 211–220. <https://doi.org/https://doi.org/10.1016/j.tecto.2006.05.042>
- Pasari, S., Simanjuntak, A. V. H., Mehta, A., Neha, & Sharma, Y. (2021). The Current State of Earthquake Potential on Java Island, Indonesia. *Pure and Applied Geophysics*. <https://doi.org/10.1007/s00024-021-02781-4>
- Pavlidou, E., van der Meijde, M., van der Werff, H., & Hecker, C. (2016). Finding a needle by removing the haystack: A spatio-temporal normalization method for geophysical data. *Computers and Geosciences*, 90, 78–86. <https://doi.org/10.1016/j.cageo.2016.02.016>
- Pavlidou, E., van der Meijde, M., van der Werff, H., & Hecker, C. (2019). Time series analysis of land surface temperatures in 20 earthquake cases worldwide. *Remote Sensing*, 11(1). <https://doi.org/10.3390/rs11010061>
- Pulinets, S. A., Ouzounov, D., Karelin, A. V., Boyarchuk, K. A., & Pokhmelnikh, L. A. (2006). The physical nature of thermal anomalies observed before strong earthquakes. *Physics and Chemistry of the Earth, Parts A/B/C*, 31(4), 143–153. <https://doi.org/https://doi.org/10.1016/j.pce.2006.02.042>
- Qiang, Z., Dian, C., Li, L., Xu, M., Ge, F., Liu, T., Zhao, Y., & Guo, M. (1999). Satellite thermal infrared brightness temperature anomaly image-short-term and impending earthquake precursors. *Science in China, Series D: Earth Sciences*, 42(3), 313–324. <https://doi.org/10.1007/BF02878968>
- Rogachev, K. A., Carmack, E. C., & Salomatin, A. S. (2000). Strong Tidal Mixing and Ventilation of Cold Intermediate Water at Kashevarov Bank, Sea of Okhotsk. *Journal of Oceanography*, 56(4), 439–447. <https://doi.org/10.1023/A:1011132507144>
- Shetty, A., Umesh, P., & Shetty, A. (2021). An exploratory analysis of urbanization effects on climatic variables: a study using Google Earth Engine. *Modeling Earth Systems and Environment*, 0123456789. <https://doi.org/10.1007/s40808-021-01157-w>
- Shi, Y., Wu, K., Zhu, X., Yang, F., & Zhang, Y. (2016). Study of relationship between wave transport and sea surface temperature anomaly (SSTA) in the tropical Pacific. *Acta Oceanologica Sinica*, 35(9), 58–66. <https://doi.org/10.1007/s13131-016-0928-4>
- Subrahmanyam, M. V. (2015). Impact of typhoon on the north-west Pacific sea surface temperature: A case study of Typhoon Kaemi(2006). *Natural Hazards*, 78(1), 569–582. <https://doi.org/10.1007/s11069-015-1733-7>
- Tamiminia, H., Salehi, B., Mahdianpari, M., Quackenbush, L., Adeli, S., & Brisco, B. (2020). Google Earth Engine for geo-big data applications: A meta-analysis and systematic review. *ISPRS Journal of Photogrammetry and Remote Sensing*, 164(March), 152–170. <https://doi.org/10.1016/j.isprsjprs.2020.04.001>
- Tronin, A. A. (2000). Thermal IR satellite sensor data application for earthquake research in China. *International Journal of Remote Sensing*, 21(16), 3169–3177. <https://doi.org/10.1080/01431160050145054>
- Tüfekçi, K., & Akman, A. Ü. (2005). Monitoring the turbidity and surface temperature changes and effects of the 17 August 1999 earthquake in the İzmit Gulf, Turkey by the Landsat TM/ETM data. *Environmental Monitoring and Assessment*, 108(1–3), 45–57. <https://doi.org/10.1007/s10661-005-3959-4>
- USGS-NEIC. (2020). *Search Earthquake Catalog*. U.S. Geological Survey-National Earthquake Information Center.
- Xiong, P., & Shen, X. (2017). Outgoing longwave radiation anomalies analysis associated with different types of seismic activity. *Advances in Space Research*, 59(5), 1408–1415. <https://doi.org/10.1016/j.asr.2016.12.011>
- Zhigalin, A. D., Zav'yalov, A. D., Mindel', I. G., Nikonov, A. A., Popova, O. G., Rogozhin, E. A., Ruzaikin, A. I., & Sevost'yanov, V. V. (2014). The phenomenon of the Sea of Okhotsk Earthquake of May 24, 2013, in Moscow. *Herald of the Russian Academy of Sciences*, 84(4), 283–291. <https://doi.org/10.1134/S1019331614040054>